Recombinant Protein L: Production, Purification and Characterization of a Universal Binding Ligand

Journal of Biotechnology 359 (2022) 108–115

Contents lists available at ScienceDirect

Journal of Biotechnology

journal homepage: www.elsevier.com/locate/jbiotec

Recombinant Protein L: Production, Purification and Characterization of a Universal Binding Ligand

Stefan Kittler [a,b,1], Julian Ebner [a,b,1], Mihail Besleaga [a], Johan Larsbrink [c], Barbara Darnhofer [d], Ruth Birner-Gruenberger [d,e], Silvia Schobesberger [f], Christopher K. Akhgar [g], Andreas Schwaighofer [g], Bernhard Lendl [g], Oliver Spadiut [a,*]

[a] Research Division Integrated Bioprocess Development, Institute of Chemical, Environmental and Bioscience Engineering, TU Wien, Gumpendorfer Strasse 1a, 1060 Vienna, Austria
[b] Alfred Gruber GmbH, Nordstrasse 6, 5301 Eugendorf, Austria
[c] Wallenberg Wood Science Center, Division of Industrial Biotechnology, Department of Biology and Biological Engineering, Chalmers University of Technology, Gothenburg, Sweden
[d] Research Division Functional Proteomics and Metabolic Pathways, Diagnostic and Research Institute of Pathology, Medical University of Graz, Stiftingtalstrasse 24, 8010 Graz, Austria
[e] Research Division Bioanalytics, Institute of Chemical Technology and Analytics, TU Wien, Getreidemarkt 9/164, 1060 Vienna, Austria
[f] Research Division Organic & Biological Chemistry, Institute of Applied Synthetic Chemistry, TU Wien, Getreidemarkt 9/163, 1060 Vienna, Austria
[g] Research Division Environmental Analytics, Process Analytics and Sensors, Institute of Chemical Technology and Analytics, TU Wien, Getreidemarkt 9/164, 1060 Vienna, Austria

ARTICLE INFO

Keywords:
Protein L
E. coli
Recombinant production
Bioreactor
Affinity ligand

ABSTRACT

Protein L (PpL) is a universal binding ligand that can be used for the detection and purification of antibodies and antibody fragments. Due to the unique interaction with immunoglobulin light chains, it differs from other affinity ligands, like protein A or G. However, due to its current higher market price, PpL is still scarce in applications. In this study, we investigated the recombinant production and purification of PpL and characterized the product in detail. We present a comprehensive roadmap for the production of the versatile protein PpL in *E. coli*.

1. Introduction

The affinity protein protein L (PpL) originates from *Finegoldia magna* (formerly *Peptostreptococcus magnus*) and was identified by Myhre and Erntell as a membrane protein (Björck, 1988; Nilson et al., 1992; Rosenthal et al., 2012). PpL has up to 5B (binding) domains, which selectively bind to kappa light chains of immunoglobulins (Igs) and, unlike protein A and G, do not interfere with the Fc region during binding (Kittler et al., 2021; Rodrigo et al., 2015; Zheng et al., 2012). In biotechnology, PpL is of high interest due to its ability not only to bind whole Igs, but also antibody fragments containing light chains, such as single chain variable fragments (scFvs) and fragments antigen binding (Fabs) (Kittler et al., 2021; Nilson et al., 1993; Rodrigo et al., 2015; Zheng et al., 2012). Different commercial versions (4 or 5B domains) are available, as the fifth binding domain has only minor effects on the binding affinity of the protein (Kittler et al., 2021). It was shown that PpL binds to kappa subtypes 1, 3 and 4, and is therefore applicable for more Ig classes compared to protein A and G (Nilson et al., 1992; Rodrigo et al., 2015). However, all three proteins are currently used in downstream processing (DSP) and bioanalytics due to their binding abilities. Ig binding proteins enable the purification of high value products (i.e. antibodies and antibody fragments) in the pharmaceutical industry, where most of the processes use protein A, G or L affinity columns as a first chromatography capture step. Other applications encompass site-specific immobilization of Igs to maintain high functionality, including enzyme-linked immunosorbent assay (ELISA) and

* Corresponding author.
E-mail addresses: stefan.kittler@tuwien.ac.at (S. Kittler), julian.ebner@tuwien.ac.at (J. Ebner), mihail.besleaga@tuwien.ac.at (M. Besleaga), johan.larsbrink@chalmers.se (J. Larsbrink), b.darnhofer@medunigraz.at (B. Darnhofer), ruth.birner-gruenberger@tuwien.ac.at (R. Birner-Gruenberger), silvia.schobesberger@tuwien.ac.at (S. Schobesberger), christopher.akhgar@tuwien.ac.at (C.K. Akhgar), andreas.schwaighofer@tuwien.ac.at (A. Schwaighofer), bernhard.lendl@tuwien.ac.at (B. Lendl), oliver.spadiut@tuwien.ac.at (O. Spadiut).
[1] These authors contributed equally to the work.

https://doi.org/10.1016/j.jbiotec.2022.10.002
Received 21 August 2022; Received in revised form 28 September 2022; Accepted 1 October 2022
Available online 4 October 2022

immunoprecipitation (Bohinski, 2000; Shen et al., 2017). Furthermore, they are used as binding ligand for surface plasmon resonance (SPR) and biolayer interferometry (BLI) to determine binding kinetics of Igs and antibody fragments (Douzi, 2017; Kittler et al., 2021; Sultana and Lee, 2015).

However, the number of applications of PpL lag behind those of protein A and G, even though the use of PpL is the only viable alternative for binding antibody fragments missing the Fc region. To our knowledge, there is no literature describing the production of PpL available to date (process mode and conditions, purification, etc.), even though recombinant PpL versions can be purchased. Furthermore, the commercial price is approximately twice as high as for protein G and even three times higher than that of protein A (Kittler et al., 2021). We hypothesize that this is caused by the lower number of approved antibody fragments on the biopharmaceutical market compared to antibodies, reducing the need of PpL.

The goal of this study was to recombinantly produce 5B domain His_6-tagged PpL in *Escherichia coli* and test its functionality in comparison with a commercially available PpL with 4B domains (purchased from Sigma-Aldrich). In the upstream process (USP), product localization (inclusion body (IB) vs. soluble) and protein quantity were investigated by altering specific substrate uptake rate (q_s) and temperature. The downstream processing aimed to obtain a high purity (>80%) without using an expensive affinity column. In this respect, the attachment of a His_6-tag presents several advantages: It enables simple DSP, composed of Immobilized Metal Affinity Chromatography (IMAC), resulting in an efficient capture step for proteins produced in soluble form (Bornhorst and Falke, 2000; Ley et al., 2011). Furthermore, the tag enables the immobilization in a specific orientation which benefits subsequent applications such as electrochemical assays, SPR and lateral flow assays (Andreescu et al., 2001; Kröger et al., 1999; Ley et al., 2011). In the last step the purified PpL was characterized to investigate any potential negative impact of the His_6-tag on the binding characteristics of the protein.

2. Material and Methods

2.1. Strain

The cultivations were performed using an *E. coli* BL21(DE3) strain transformed with a pET-24a(+) plasmid carrying the codon-optimized gene for the 5B domain PpL (GenBank accession no. AAA67503) with a C-terminal His_6-tag (restriction sites: *Nhe*I/*Xho*I). The encoded PpL has a theoretical size of 41.98 kDa and a theoretical pI of 4.82 (supplementary information: 1. Sequencing Result). The sequence for the 5B domains originates from *F. magna* and was adapted from ProSpec (PROTEIN-L, 2019).

2.2. Media

The bioreactor cultivations were carried out using a defined medium described by DeLisa et al. (DeLisa et al., 1999), supplemented with 0.02 g/L kanamycin to prevent plasmid loss (Table 1). Glycerol was used as sole carbon source since recent results showed that this can result in higher product titers due to a higher amount of accessible energy (Kopp et al., 2017).

2.3. Bioreactor Cultivations

For pre-culture, 500 mL of DeLisa medium (Table 1) in a 2500 mL high yield shake flask were inoculated with 1.5 mL frozen bacterial stock. The pre-culture was grown at 37 °C and 230 rpm in an Infors HR Multitron incubator (Infors, Bottmingen, Switzerland) for 16 h. The cultivations were carried out in a DASGIP parallel reactor system (Eppendorf, Hamburg, Germany) with four vessels having 2 L working volume each. The culture broth was aerated with 2 L/min and stirred at 1400 rpm. The pH was monitored with an Easyferm electrode (Hamilton, Reno, NV, USA) and kept constant at 6.7 via addition of NH_4OH (12.5%). The dissolved oxygen was monitored using a Visiferm fluorescence dissolved oxygen electrode (Hamilton, Reno, NV, USA) and kept above 30% by supplying a mixture of pressurized air and pure oxygen if necessary. Off-gas was monitored using a DASGIP-GA gas analyzer (Eppendorf, Hamburg, Germany). The temperature was controlled with a heat jacket and cooling finger and kept at 37 °C for the batch and at 35 °C during the non-induced fed-batch phase. For process control and monitoring the DAS-GIP-control system (DASware-control) was used. The batch phase (volume = 1 L) was started by inoculating the reactor with 10% (v/v) of the pre-culture. Once all glycerol was depleted, as indicated by a drop of the CO_2 signal and vice versa a rise in the dO_2 signal, substrate was fed to reach a cell dry weight concentration of approx. 25 g/L. After the fed-batch, expression of PpL was induced by addition of Isopropyl β-D-1-thiogalactopyranoside (IPTG) to a final concentration of 0.5 mM (induced fed-batch). During the induction phase, the specific substrate uptake rate (q_s) and temperature were altered using a design of experiment (DoE) approach. These process parameters have been shown to be crucial factors for protein quantity and localization (IB vs. soluble) (Kopp et al., 2017; Slouka et al., 2018). During the induced fed-batch, samples were drawn every two hours to monitor product formation. The factor q_s was adjusted at the start of induction and was altered in the range of 0.1 g/g/h to 0.5 g/g/h. The temperature was investigated in a range of 27–35 °C, while the center-point conditions (CP) (q_s = 0.3 g/g/h; T = 31 °C) were performed three times to investigate reproducibility. We decided to perform a central composite circumscribed design to adequately describe potential quadratic interactions. In a first step the product localization and feasibility of a tunable production of IB or soluble PpL was investigated. For the design of DoE the volumetric product concentration in g/L was chosen as process response. The software MODDE 10 (Sartorius. Göttingen, Germany) was used for model design and to develop a multilinear regression model describing volumetric titer of PpL as a function of q_s and temperature over the induction time.

Table 1
DeLisa medium used for all cultivation phases. 0.02 g/L kanamycin were added for all phases.

	Pre-culture	Batch	Feed	
Component	Concentration [g/L]			Sterilization
Citric acid	13.3		–	autoclave
$(NH_4)_2HPO_4$	4		–	
Citric acid	1.7		–	
$MgSO_4$0.7 H_2O (stock 500 x)	1.2		10.00	autoclave
Fe(III) citrate (stock 100 x)	0.1		0.02	autoclave
EDTA (stock 100 x)	0.0084		0.0065	autoclave
$Zn(CH_3COO)_2{\cdot}H_2O$ (stock 200 x)	0.013		0.008	filter sterile
TE[a] (stock 200 x)	5 mL/L		7.27 mL/L	filter sterile
Thiamine HCl (stock 1000 x)	0.0045		–	filter sterile
Glycerol	8	20	400	autoclave

[a] TE stock: $CoCl_2$0.6 H_2O (2.5 mg/L); $MnCl_2$0.4 H_2O (15 mg/L); $CuCl_2$0.2 H_2O (1.2 mg/L); H_3BO_3 (3 mg/L); $Na_2MoO_4$0.2 H_2O (2.5 mg/L)

2.4. Bioreactor Cultivation Analytics

2.4.1. Biomass

Biomass was quantified via optical density by measuring OD_{600} using a UV/VIS photometer (Genisys 20, Thermo Scientific, Waltham, MA, USA) to monitor biomass growth during the process. Additionally, dry cell weight (DCW) was determined gravimetrically by centrifuging 1 mL of culture broth (9000 rcf, 10 min), subsequently washing the pellet with 0.9% (w/v) NaCl and centrifuging again. Afterwards the pellets were dried at 105 °C for 72 h.

2.4.2. Metabolite Analysis

The concentration of glycerol in the supernatant was analyzed via high performance liquid chromatography (HPLC) (UltiMate 3000; Thermo Fisher, Waltham, MA) using a Supelcogel C-610 H column (Supelco, Bellefonte, PA, USA) (Kopp et al., 2017). For this method 0.1% H_3PO_4 with a constant flow rate of 0.5 mL/min was used as eluent. The sugars were detected and quantified using respective standards, by a refractive index detector (Shodex RI-101, Ecom, Prague, Czech Republic) (Kopp et al., 2017). The q_s was calculated according to Eq. 1, taking accumulated glycerol into account.

$$q_s \left[\frac{g}{gh}\right] = \frac{V_{in,feed,\Delta t}\,[L] * c_{feed}\left[\frac{g}{L}\right] - V_{reactor,t_i}\,[L] * c_{acc,t_i}\left[\frac{g}{L}\right]}{\Delta t\,[h] * X_{\Delta t}\,[g]} \quad (1)$$

$q_s\left[\frac{g}{gh}\right]$ … specific substrate uptake rate.

$V_{in,feed,\Delta t}[L]$ … feed volume in timespan Δt.

$c_{feed}\ \left[\frac{g}{L}\right]$ … glycerol concentration in the feed (400 g/L).

$V_{reactor,t_i}[L]$ … reactor volume at time point i.

$c_{acc,t_i}\left[\frac{g}{L}\right]$ … concentration of glycerol in the supernatant at time point i.

$\Delta t[h]$ … timespan ($t_i - t_{i-1}$) for the calculation of q_s.

$X_{\Delta t}\ [g]$ … average biomass in the reactor in the timespan Δt.

2.4.3. Product Analysis

For determining the PpL concentration, 10 mL of the cultivation broth were centrifuged at 9000 rcf for 10 min at 4 °C. The supernatant was discarded and the product samples were stored at − 20 °C until further use. The cell pellet was suspended in 40 mL lysis buffer (100 mM Tris, 10 mM EDTA, pH = 7.4) and homogenized using a high-pressure homogenizer at 1200 bar for 7 passages (PandaPLUS, Gea AG, Germany). Subsequently, the cell suspension was centrifuged at 20,380 rcf for 20 min at 4 °C, and supernatant and IB pellet were further analyzed as described in the sections below.**a) SDS-PAGE**For SDS-PAGE, Mini-PROTEAN® TGX Stain-Free™ (BioRad, Hercules, CA, USA) gels were used. The IB pellet were dissolved in 1x Laemmli buffer containing 100 µL ß-mercaptoethanol (reducing conditions) (Laemmli, 1970). The soluble fraction was mixed in a 1–2 ratio with 2x Laemmli buffer. All samples were incubated at 95 °C for 10 min and subsequently spun down. Five µL of a protein molecular weight standard (precision plus protein standard dual color, BioRad) and 10 µL of each sample were loaded in the respective wells. The gel was run at 180 V for 30 min. Staining was performed using Coomassie brilliant blue and gels were analyzed using a Gel Doc (Universal Hood II, BioRad, Hercules, CA, USA) and the ImageLab software (Version 6.0.1, BioRad, Hercules, CA, USA).**b) HPLC**Reversed Phase-HPLC:The product concentration was determined using a BioResolve reversed phase (RP) Polyphenyl column (dimensions 100 × 3 mm, particle size 2.7 µm) (Waters Corporation, MA, USA) equipped with a pre-column (3.9 × 5 mm, 2.7 µm (Kopp et al., 2020). Eluent A was ultrapure water (MQ) and eluent B was acetonitrile, both supplemented with 0.1% (v/v) trifluoroacetic acid. A sample volume of 2 µL was injected. The flow was kept constant at 0.4 mL/min and the measurement performed at 70 °C. A detailed description of the used method is given by Kopp et al. (Kopp et al., 2020). The soluble fractions were filtered with a 0.2 µm syringe filter (CHROMAFIL® Xtra PVDF-20/25, Pall, New York, USA), while the IB pellets were first solubilized with 7.5 M guanidine hydrochloride, 62 mM Tris and 100 mM DTT at pH = 8 and filtered afterwards. To determine the protein concentration, BSA (bovine serum albumin) standards with concentrations between 0.1 and 2 g/L were measured. Size Exclusion Chromatography-HPLC:PpL concentration and purity during the DSP was measured using a size exclusion chromatography (SEC)-HPLC method. A BEH 200 A SEC 1.7 µm 4.6 × 300 mm, 3.5 µm (Waters Corporation, MA, USA) column was run isocratically with SEC buffer (80 mM phosphate, 250 mM KCl, pH = 6.8) (Kittler et al., 2020). The method run time was 18 min with a flow rate of 0.5 mL/min and an injection volume of 2 µL was used. Column temperature was kept constant at 25 °C and absorbance was recorded at 280 nm and 214 nm. For quantification purposes, BSA protein standards were measured between 0.125 and 2 g/L and PpL concentrations calculated based on the calibration curve.

2.5. Downstream Processing

The biomass of each cultivation was harvested 12 h after induction, centrifuged at 17,000 rcf, 4 °C, 30 min and the biomass pellet stored at − 20 °C until further use. For the described DSP protocol, biomass produced at $q_s = 0.3$ g/g/h and T = 31 °C was used. For preparative chromatography, an ÄKTA pure™ system (Cytiva Life Sciences, MA, USA) was used, monitoring conductivity and UV absorbance at three wavelengths (280 nm, 260 nm, 214 nm).

The DSP comprised the following steps:

- Cell lysis via high pressure homogenization
- Capture via IMAC chromatography
- Purification via anion exchange chromatography (AEC)

2.5.1. High Pressure Homogenization

In order to release intracellularly produced soluble PpL, cell lysis was performed via high pressure homogenization using a PandaPLUS (Gea AG, Germany). Frozen biomass was resuspended in Buffer A (50 mM phosphate, pH = 7.4) containing protease inhibitor (cOmplete™ Mini, EDTA-free, Roche, Switzerland) to a final concentration of 13 g DCW/L buffer A. Homogenization was performed at 1200 bar for 7 passages and the homogenized sample was kept at 4 °C afterwards. In order to separate cell debris from the soluble fraction containing PpL, the sample was centrifuged at 20,380 rcf for 20 min at 4 °C. The supernatant was used in the following chromatography step and the pellet discarded.

2.5.2. Capture Chromatography: IMAC

As a capture step for the His_6-tagged PpL, a 5 mL HiTrap™ IMAC FF (Cytiva Life Sciences, MA, USA) with a flowrate of 0.2 column volumes (CV)/min was used. The column was equilibrated with buffer A (50 mM phosphate, pH = 7.4) until all signals were stable. The supernatant (35 mL) after homogenization was loaded onto the column, followed by a wash step with 4 CVs of buffer A. Elution was performed using a step gradient with 40% buffer B (50 mM phosphate, 500 mM imidazole, pH = 7.4). During elution, fractions of 1 mL were collected, pooled based on the UV 280 nm signal and analyzed for their respective concentration and purity using SEC-HPLC.

2.5.3. Purification Chromatography: AEC

As purification step, a 1 mL Hitrap™ Capto Q (Cytiva Life Sciences, MA, USA) column with a flowrate of 1 CV/min was used. The column was equilibrated with buffer A (50 mM phosphate, pH = 7.4). The pooled fractions containing PpL obtained from the capture chromatography step (IMAC) were used as load (6 mL load volume) (Cytiva, 2021a, 2021b). After loading was completed, the column was washed with 5 CVs buffer A. PpL was eluted using a step gradient with 25% buffer C (50 mM phosphate, 1 M NaCl, pH = 7.4). As for IMAC, fractions of 1 mL were collected, pooled based on the UV 280 nm signal and analyzed for their respective concentration and purity using SEC-HPLC.

2.6. Characterization and Protein Functionality

2.6.1. Mass Spectrometry

The primary structure and mass of the purified His_6-tagged PpL was confirmed using digestion followed by LC/MS (liquid chromatography/mass spectrometry). Additionally, the total mass of the produced PpL and the commercial PpL (for comparison) was measured using intact protein mass spectrometry. A detailed description of the performed

measurements can be found in the supplementary information (supplementary information: 6. Mass spectrometry).

2.6.2. Infrared Spectroscopy

Both PpL variants were measured using laser-based mid-infrared spectroscopy to obtain structural information. A detailed description of the applied external cavity-quantum cascade laser (EC-QCL) setup has previously been reported (Akhgar et al., 2020). Briefly, the laser (Hedgehog, Daylight Solutions Inc., San Diego USA) was operated in a tuning range between 1470 cm^{-1} and 1730 cm^{-1} with a scan speed of 3600 cm^{-1} and pulse rate and width of 1 MHz and 200 ns, respectively. The IR light was attenuated by optical filters, divided into two beams and directed into a two-path transmission flow cell with a path length of 26 μm. Approximately 500 μL of sample solution were injected into the signal cell, while the reference cell was filled with the pure buffer solution. The intensity of both beams was detected by a thermoelectrically cooled mercury cadmium telluride balanced detector (Vigo System S.A., Poland) to compensate the noise introduced by the EC-QCL. A previously described pre-processing routine (Schwaighofer et al., 2018), including similarity index evaluation, scan averaging (300 single scans = 45 s acquisition time) and fast Fourier transform (FFT) filtering, was applied in order to obtain the final protein spectra with a spectral resolution of 2.6 cm^{-1}.

2.6.3. Surface Plasmon Resonance

Surface plasmon resonance spectroscopy (SPR) was performed at the core facility at the University of Natural Resources and Life Sciences in Vienna. For the measurement, a Bioacore T200 (Cytiva Life Sciences, MA, USA) was used. For measuring the binding affinity of both PpL samples, a commercial protein A chip was used. In the first step, a 10 μg/mL Herceptin solution was applied to bind the antibody to the protein A chip. Subsequently, to monitor the binding affinity, different PpL concentrations (0.617, 1.85, 5.55, 16.6, and 50 nM respectively) were loaded for 10 min. The flow rate for all loading steps was 10 μL/min. The general running buffer was HBS-EP buffer (Cytiva Life Sciences, MA, USA). The obtained RPU (response) was plotted versus the time and fitted with a one site saturation model (Eq. 1) using Sigma plot (Systat Software GmbH) to determine the response at equilibrium. The RPU at equilibrium of all measurements was then plotted against the respective concentration and fitted with a one site saturation equation to determine the K_D value (Eq. 2) (Moscetti et al., 2017; Sparks et al., 2019).

$$y = \frac{B_{max} * x}{K_D + x} \tag{2}$$

y … y – value e.g. response of the SPR measurement B_{max} … maximal y-value x … x – value e.g. concentration of the analyte K_D … analyte concentration at $B_{max}/2$.

2.6.4. Structure Analysis

Finally, the 3D structure of PpL was predicted using AlphaFold (Jumper et al., 2021; Varadi et al., 2022). For the analysis, the full amino acid sequence including the His6-tag was used and the prediction computed using the Alvis cluster within the Chalmers Centre for Computational Science and Engineering (C3SE), Sweden.

2.6.5. ELISA

To evaluate the functionality of the purified PpL, the purified protein was conjugated to recombinant horseradish peroxidase (HRP) and ELISA was performed. A detailed description of the protocol for conjugation, which was adapted from Nygren et al. and Molin et al. is given in the supplementary information (supplementary information: 2. ELISA Conjugation) (Molin So Fau - Nygren et al., 1978a, 1978b; Nygren et al., 1981).

For the ELISA, 100 μL Herceptin (200 μg/mL) in phosphate buffered saline (PBS, pH = 7.4) was incubated at 4 °C in high binding ELISA plates (Greiner Bio-One, Kremsmünster, Austria) for 16 h. Afterwards, the Herceptin solution was removed and the wells were washed four times with PBS containing 0.05% Tween20 (=wash buffer). Subsequently, to block open binding positions, the wells were incubated with 200 μL 1% BSA in PBS (=blocking solution) for 60 min at RT. Then the wells were washed again four times with wash buffer. Subsequently, the respective detection complex with a concentration of 0.2 μg/mL was incubated at RT for 30 min (Table 2). The solution in the wells was discarded and wells were washed seven times with wash buffer to remove non-specifically bound HRP.

Bound HRP-PpL conjugates were quantified immediately after the last washing step using a S2,2′-azino-bis(3-ethylbenzothiazoline-6-sulfonic acid) (ABTS) assay. 180 μL of 8 mM ABTS in 50 mM phosphate-citrate buffer, pH = 5, were pipetted in each well and the reaction was started by adding 20 μL 10 mM H_2O_2. The change of absorbance at 420 nm was monitored for 45 min using a Tecan plate reader (Spark®, Tecan, Männedorf, Switzerland) at 30 °C. For each well, the volumetric activity was calculated according to Eq. 3.

$$A\left[\frac{U}{mL}\right] = \frac{V_{total}[\mu L] * \Delta A/\min * dilution}{V_{sample}[\mu L] * d[cm] * \varepsilon[mM^{-1} * cm^{-1}]} \tag{3}$$

V_{total} [μL] … total volume in well.
ΔA/min … change in absorption (ΔAbs 420 nm/min).
Dilution … dilution of the sample.
V_{sample} [μL] … volume of sample.
d [cm] … length of the beam path through the cuvette (d = 0.58 cm).
ε [mM^{-1} *cm^{-1}] … extinction coefficient (ε_{420} = 36 mM^{-1} *cm^{-1}).

3. Results and Discussion

3.1. Production and Purification of Recombinant Protein L

The goal of this study was to develop a production process for recombinant PpL that enables production of a high amount of biologically active protein with high purity (>80%). The investigated variables in the USP and DSP are listed in Table 3.

For the recombinant production of His_6-tagged PpL, the specific substrate uptake rate and temperature (q_s, T) were investigated in a DoE approach. In previous studies it was shown that these process variables influence localization (IB or soluble) and quantity of produced recombinant protein (Kopp et al., 2017; Slouka et al., 2018). For all tested fermentation conditions, an excess of soluble PpL compared to IBs (9 g/L to <0.5 g/L) was observed (supplementary information: Fig. S1). Since PpL originates from a bacterial host, we believe that expression has a low burden on *E. coli* due to low protein complexity (no disulfide bridges or other post-translational modifications) and therefore only low amounts of IB were produced (Bhatwa et al., 2021). As depicted in Fig. 1a, high specific substrate uptake rates (≥0.5 g/g/h) led to an increase of the volumetric product titer in the beginning of the induction phase. However, after four to six hours, glycerol started to accumulate (data not shown) as the biomass growth stopped (DCW decreased) and the volumetric productivity declined. The observed drop in the specific growth rate correlated with the mentioned accumulation of glycerol, caused by a high metabolic stress using a q_s higher than 0.5 g/g/h. Lower temperatures (25.3 °C and 27 °C) did not increase the amount of

Table 2
Tested combination of samples and conjugation-complex. HRP: horseradish peroxidase; PpL: protein L; BSA: bovine serum albumin.

Immobilized protein	Detection complex
Herceptin	HRP
Herceptin	PpL
Herceptin	PpL-HRP
BSA	PpL-HRP

Table 3
Overview of investigated factors in the production process of recombinant protein L. USP: upstream processing; DSP: downstream processing; q_s: specific substrate uptake rate; IMAC: immobilized metal affinity chromatography.

Unit operation	Factors	Range
USP	q_s	0.1 g/g/h – 0.5 g/g/h
	Temperature	27–35 °C
DSP - IMAC	NaCl	0 mM or 500 mM

PpL, independent of the adjusted q_s. The CP conditions (q_s = 0.3 g/g/h, temperature 31 °C) resulted in an almost linear increase of the volumetric titer, while higher temperatures did not lead to an increase of product formation.

The regression model for the volumetric titer showed that longer induction time had a positive influence on productivity (Fig. 1b). Furthermore, increasing temperature led to an increase of the volumetric titer, while the quadratic terms of all tested parameters had a negative impact on product formation (supplementary information: Fig. S2). The highest volumetric product titer (>9 g/L) was achieved at a q_s = 0.3 g/g/h, a temperature of 31 °C and an induction time of 12 h, leading to a specific product titer of 0.17 g/g with a final biomass concentration of 55 g DCW/L (process data: supplementary information: Figs. S3 and S4).

After cell lysis, the His_6-tagged PpL was purified to achieve purities

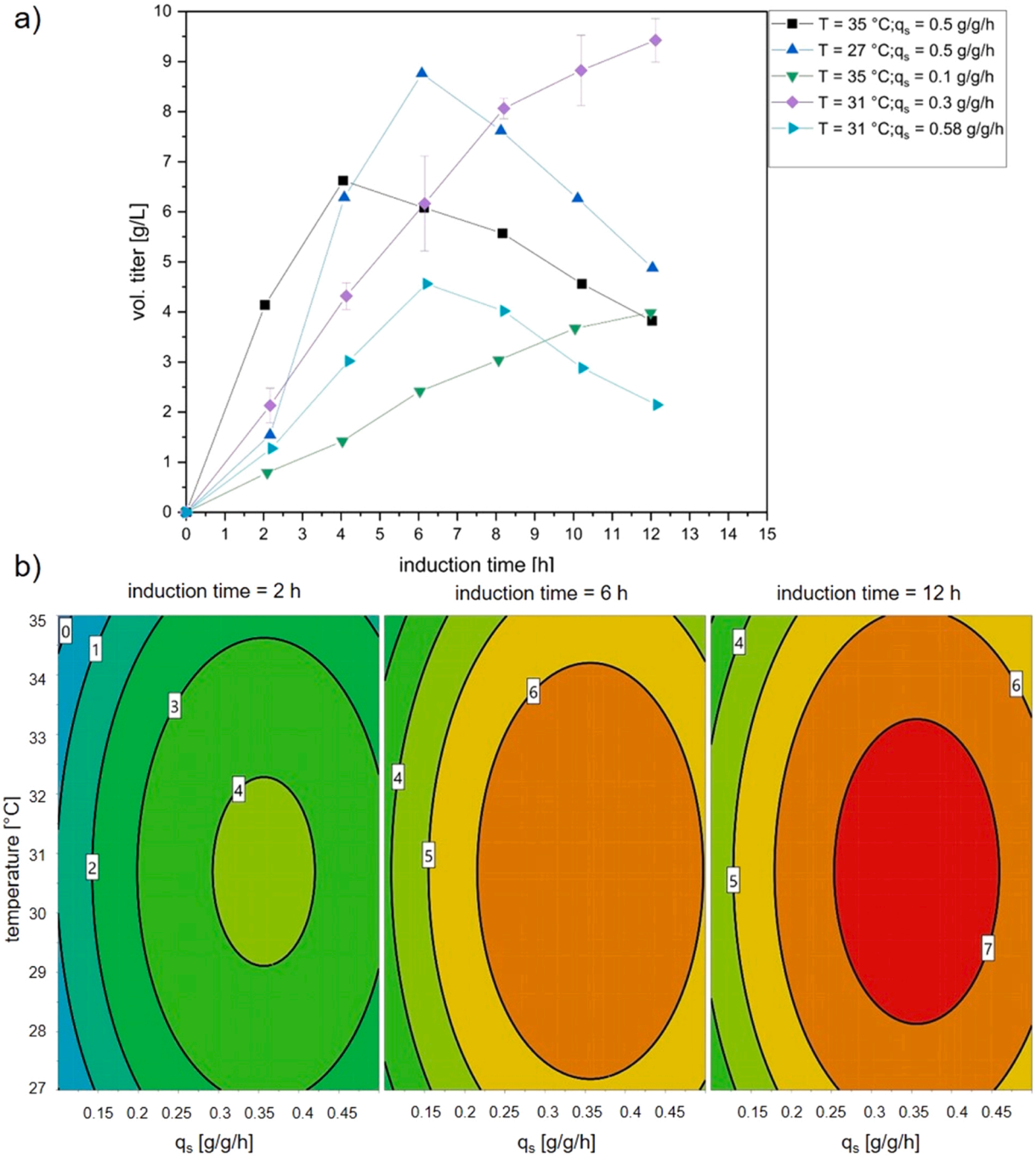

Fig. 1. a: Time resolved trend of volumetric titer [g/L] of performed cultivations according to the design of experiment (DoE). b: Contour plot of the volumetric titer [g/L]. The optimum in the tested design space is at a specific substrate uptake rate (q_s) = 0.3 g/g/h and temperature 31 °C after 12 h. These conditions led to a product concentration of about 9 g/L.

similar to the commercial PpL (i.e. 80%, determined by SEC). A standard protocol for IMAC, including 20 mM imidazole in the sample and the binding buffer, led to unexpectedly low recoveries (<30%, data not shown). In order to improve binding capacity and recovery, sample and binding buffers were prepared without imidazole. This adaptation resulted in improved recovery (59%) and purity (67%). Still, a second chromatography step was required to reach the targeted purity of > 80%. Due to the pI of 4.82, an anion exchange chromatography (AEC) step was chosen. However, the used salt (500 mM NaCl) in the IMAC buffers requires a buffer exchange to ensure sufficient binding in the subsequent AEC step. Therefore, we investigated whether NaCl can be omitted in the IMAC step without negative effects on recovery and purity. Summarized in Table 4, the final process using IMAC buffers without salt showed increased recovery and purity, resulting in a final PpL purity of 92% and a final yield of 5 g PpL / L fermentation broth (57%) after the second AEC step. As an additional advantage, the eluate of the capture step (IMAC) could directly be used to load the column in the second purification step, circumventing additional unit operations such as e.g. pH-adjustment or buffer exchange (Cytiva, 2021a, 2021b). The presented process might be a viable alternative to industrial production processes in which far more expensive Ig containing resins are used for the capture step (Cytiva). Furthermore, the purified 5B domain His_6-tagged PpL had a higher purity (92%) compared to the commercial protein (80%). However, it is important to mention that DNA and endotoxin concentrations were not analyzed.

3.2. Protein Structure and Functionality Analysis

First, the primary structure of both PpL variants (TU Wien: 5B domain His_6-tagged PpL and Sigma-Aldrich: 4B domain PpL) was confirmed using enzymatic digestion followed by LC/MS. However, due to the existence of repetitive B domains, the exact mass of the proteins could not be determined by analyzing the fragments. For this purpose, whole protein LC/MS was performed of each PpL variant. The 5B domain His_6-tagged PpL, had a mass of 41816 Da (supplementary information: Fig. S5), while the commercial 4B domain PpL (one binding domain less) had a mass of 36038 Da (supplementary information: Fig. S6). Moreover, for both PpL variants, a distribution of different mass fragments was observed. This size heterogeneity has been reported for different Ig-binding proteins of Gram-positive bacteria (Kastern et al., 1992).

Laser-based mid-IR spectroscopy was applied to record absorbance spectra across the amide I (1600–1700 cm^{-1}) and amide II (1500–1600 cm^{-1}) bands, since these represent the most important wavenumber regions for protein secondary structure determination (Barth, 2007). Compared to conventional Fourier-transform infrared (FTIR) instrumentation, EC-QCLs operate at significantly higher spectral power densities, thus allowing the application of larger optical path lengths that lead to improved robustness and sensitivity (Schwaighofer and Lendl, 2020). Fig. 2a shows a comparison of PpL from Sigma-Aldrich (4B domains) and PpL produced here (TU Wien; 5B domains His_6-tagged). Positions and shapes of the IR absorbance bands show excellent comparability between the spectra. The maxima at 1640 cm^{-1} in the amide I region, as well as the broad amide II bands at approximately 1550 cm^{-1} indicate a high share of β-sheet secondary structure (Barth, 2007).

Table 4
Recovery and purity of the His_6-tagged PpL comparing the IMAC runs with and without 500 mM NaCl.

Step	Recovery [%]	Purity [%]
Capture (IMAC) with NaCl	66	45
Whole DSP	44	72
Capture (IMAC) without NaCl	49	67
Whole DSP	57	92

For testing functionality and binding affinity, SPR measurements were performed to determine the K_D value of both PpL variants. However, PpL has a very high affinity to Igs and antibody fragments, indicated by a small K_D and a slow dissociation reaction. Therefore, the dissociation could not be determined with the used experimental set up, since no steady state was achieved (data not shown). As an alternative approach, the maximum signals for steady state conditions were calculated based on a one site saturation model. In Fig. 2b the maximum fitted response (RPU) for each tested concentration is plotted against the respective concentration (Moscetti et al., 2017; Sparks et al., 2019). The obtained values were fitted again using a one site saturation model to determine the K_D values (Fig. 2b).

The determined K_D value for the recombinant 5B His_6-tagged PpL variant ($K_D = 2.93 \times 10^{-10}$ M) was lower than for the commercial 4B domain PpL ($K_D = 1.55 \times 10^{-9}$ M). This can likely be attributed to the additional B domain in the construct, which slightly increases the affinity (Kastern et al., 1992; Kittler et al., 2021).

After similarity of the secondary structure was validated for both variants and the functionality was demonstrated, the tertiary structure of the 5B His_6-tagged PpL variant was modeled using AlphaFold (Jumper et al., 2021; Varadi et al., 2022). Since no amino acid sequence was available for the commercial PpL variant, a comparison of the modeled structures was not possible. However, the single B domains could be predicted with high confidence and are in accordance with literature (Kittler et al., 2021; Wikstroem et al., 1994). The linkers between the binding domains were found to have lower prediction scores and are most likely flexible and without a defined structures (Fig. 3, supplementary information: Fig. S7). These linkers as well as the unstructured N- and C- terminal ends of the protein (the latter incorporating the His_6-tag) could be susceptible to some proteases, possibly explaining the size heterogeneity observed in mass analysis and the low recovery during the capture step (IMAC) (Shen et al., 1991).

3.3. Application of Protein L in an ELISA

For the purpose of using PpL in an ELISA, both PpL variants were conjugated to recombinant HRP and used to detect Herceptin. First, solely the HRP activity without the binding to Herceptin was measured. The recombinant His_6-tagged 5B domain PpL conjugate showed an activity of $6.82 \pm 0.27 \times 10^3$ U/mol, which was similar to the 4B domain conjugate PpL that showed an activity of $7.49 \pm 0.91 \times 10^3$ U/mol. However, it was expected that the 5B domain PpL would exhibit a higher amount of conjugated HRP due to the higher number of primary amines (e.g. lysine), which act as conjugation partners. However, we assume that these additional primary amines were not accessible due to their position within the binding domains, resulting in similar amounts of conjugated HRP. In the ELISA, the His_6-tagged PpL with 5B domains achieved a volumetric activity of 3.99 ± 0.86 U/mL, while for the commercial PpL (Sigma-Aldrich) with 4B domains showed an activity of 4.96 ± 0.92 U/mL. Conjugation of PpL to HRP without loss of activity and detection of an antibody was thus possible for both variants, showing that the tested HRP-PpL complex can be successfully used for ELISAs applied as in-process control e.g. in the early DSP or for refolding processes.

4. Conclusion

In this study we were able to successfully produce and purify recombinant His_6-tagged PpL with 5B domains in *E. coli* with a final product yield of 5 g product per L fermentation broth. The produced protein was characterized and compared to a commercially available PpL regarding secondary structure and activity (Table 5). The initial DSP resulted in unexpectedly low recoveries and purities, but these could be significantly improved by optimization of the IMAC capture step and performing a second AEC step. The results from the performed MS indicate a size heterogeneity of PpL, which could possibly explain the

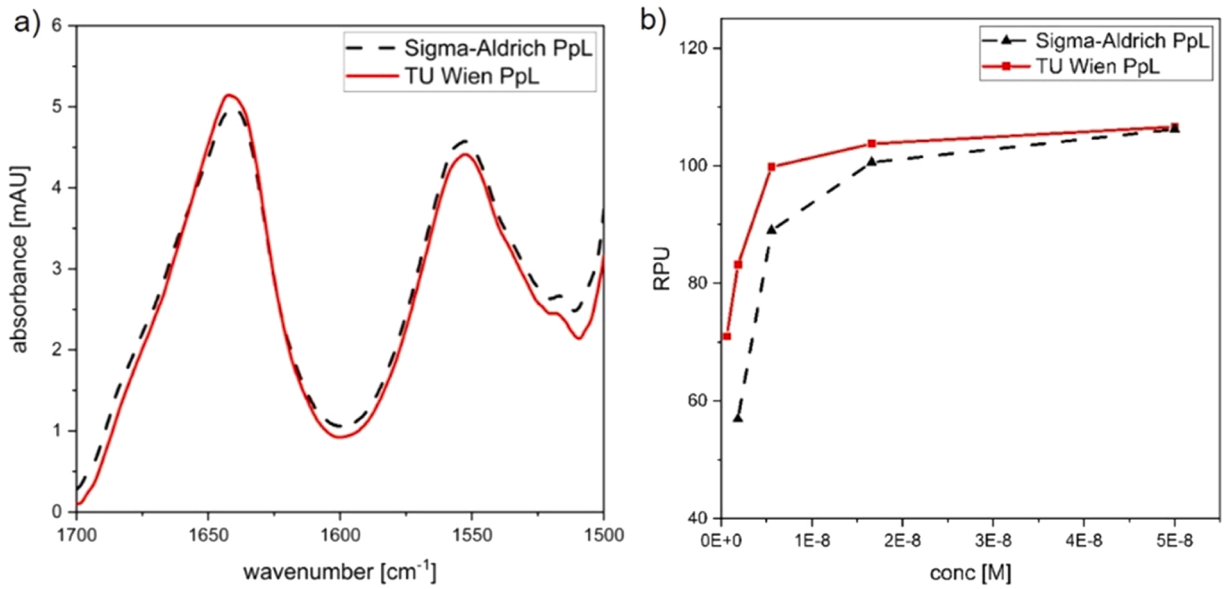

Fig. 2. a: IR spectrum of both protein L (PpL) variants. Both 4B domain and 5B domain His_6-tagged PpL, from Sigma-Aldrich and TU Wien, respectively, show highly similar absorbance spectra indicating comparable secondary structure. b: Results of the SPR measurement of both protein L (PpL) variants. The calculated saturation values for each concentration is plotted against the respective concentration. The curve was fitted with a one-site saturation equation to determine the K_D value. 4B domain PpL (Sigma-Aldrich PpL) $K_D = 1.5 \times 10^{-9}$ M; 5B domain His_6-tagged PpL (TU Wien PpL): $K_D = 2.93 \times 10^{-10}$ M.

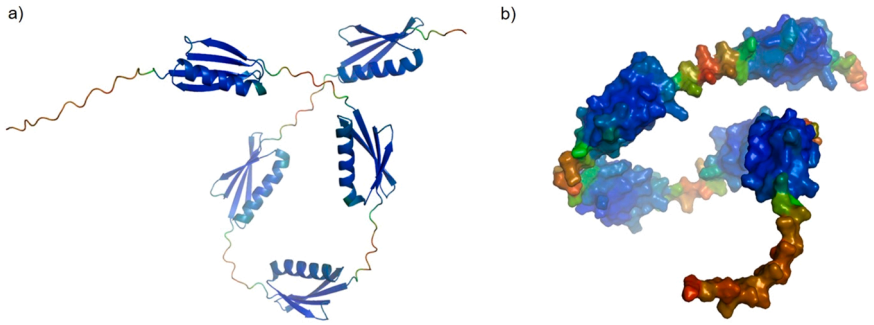

Fig. 3. a) Cartoon models colored by the prediction score, red-green-blue, from low to high, with the N-terminus on the left. b) Space-fill model of His_6-tagged protein L, colored as in a), and with the N-terminus at the bottom. The structure of the B domains are confidently predicted, while the structure of the linkers and termini cannot be predicted reliably and are likely flexible in solution.

Table 5
Summary of the results of the structural and functionality analysis of both protein L (PpL) variants. mAb: monoclonal antibody.

	TU Wien PpL	Sigma-Aldrich PpL
Mass [Da]	41816	36038
Structure of single B domain	4 beta sheets + 1 alpha helix	4 beta sheets + 1 alpha helix
B domains	5	4
K_D [M]	2.93×10^{-10}	1.55×10^{-9}
Application in ELISA	Detection of mAb possible	Detection of mAb possible

still somewhat low overall recoveries. The structural analysis revealed unstructured protein parts that could be susceptible to cleavage, which would then result in different protein sizes and loss of the purification tag. We believe that further studies focusing on the structure of PpL will help to understand the observed results. Nevertheless, the secondary structure of the produced PpL was similar to the commercial variant with 4B domains. Furthermore, it was shown that the produced PpL is functional and active, without being negatively influenced by the HIS_6-tag and the obtained K_D value was lower compared to the 4B domain PpL. Additionally, the application in an ELISA detecting Herceptin using a PpL-HRP conjugate was successful.

Funding

This research was funded by the Austrian Research Promotion Agency (FFG) (874206). The authors acknowledge the TU Wien Bibliothek for financial support through its Open Access Funding Program.

CRediT authorship contribution statement

SKI and JEB conducted most of the experiments and wrote the draft, MBE supported in the bioprocessing tasks, JLA did the protein model, BDA and RBG performed mass spectrometry, SSC assisted in the ELISA experiments, CAK, ASC and BLE did spectroscopic analyses, OSP initiated and supervised the study, secured funding and corrected the draft.

Declaration of Competing Interest

The authors declare that they have no known competing financial interests or personal relationships that could have appeared to influence the work reported in this paper.

Data Availability

Data will be made available on request.

Acknowledgments

Alfred Gruber GmbH is gratefully thanked for supporting the research and being project partner. This project was further supported by EQ-BOKU VIBT GmbH and the BOKU Core Facility Biomolecular & Cellular Analysis. Furthermore, we thank Karolina Golab for performing the conjugation and ELISA experiments.

Appendix A. Supporting information

Supplementary data associated with this article can be found in the online version at doi:10.1016/j.jbiotec.2022.10.002.

References

Akhgar, C.K., Ramer, G., Żbik, M., Trajnerowicz, A., Pawluczyk, J., Schwaighofer, A., Lendl, B., 2020. The next generation of IR spectroscopy: EC-QCL-Based Mid-IR transmission spectroscopy of proteins with balanced detection. Anal. Chem. 92, 9901–9907.

Andreescu, S., Magearu, V., Lougarre, A., Fournier, D., Marty, J.L., 2001. Immobilization of enzymes on screen-printed sensors via an histidine tail. Application to the detection of pesticides using modified cholinesterase. Anal. Lett. 34, 529–540.

Barth, A., 2007. Infrared spectroscopy of proteins. Biochim. Et Biophys. Acta (BBA) - Bioenergy 1767, 1073–1101.

Bhatwa, A., Wang, W., Hassan, Y.I., Abraham, N., Li, X.-Z., Zhou, T., 2021. Challenges associated with the formation of recombinant protein inclusion bodies in escherichia coli and strategies to address them for industrial applications. Front. Bioeng. Biotechnol. 9, 65.

Björck, L., 1988. Protein L. A novel bacterial cell wall protein with affinity for Ig L chains. J. Immunol. 140, 1194–1197.

Bohinski, R.C., 2000. Immunoprecipitation of serum albumin with protein A-sepharose: a biochemistry laboratory experiment. J. Chem. Educ. 77, 1460.

Bornhorst, J.A., Falke, J.J., 2000. Purification of proteins using polyhistidine affinity tags. Methods Enzymol. 326, 245–254.

Cytiva, ⟨https://www.cytivalifesciences.com/en/at⟩ (accessed 10 August 2021a).

Cytiva, (2021b) Tips for successful ion exchange chromatography.

DeLisa, M.P., Li, J., Rao, G., Weigand, W.A., Bentley, W.E., 1999. Monitoring GFP-operon fusion protein expression during high cell density cultivation of Escherichia coli using an on-line optical sensor. Biotechnol. Bioeng. 65, 54–64.

Douzi, B., 2017. Protein–protein interactions: surface plasmon resonance. In: Journet, L., Cascales, E. (Eds.), Bacterial Protein Secretion Systems: Methods and Protocols. Springer, New York, New York, NY, pp. 257–275.

Jumper, J., Evans, R., Pritzel, A., Green, T., Figurnov, M., Ronneberger, O., Tunyasuvunakool, K., Bates, R., Žídek, A., Potapenko, A., Bridgland, A., Meyer, C., Kohl, S.A.A., Ballard, A.J., Cowie, A., Romera-Paredes, B., Nikolov, S., Jain, R., Adler, J., Back, T., Petersen, S., Reiman, D., Clancy, E., Zielinski, M., Steinegger, M., Pacholska, M., Berghammer, T., Bodenstein, S., Silver, D., Vinyals, O., Senior, A.W., Kavukcuoglu, K., Kohli, P., Hassabis, D., 2021. Highly accurate protein structure prediction with AlphaFold. Nature 596, 583–589.

Kastern, W., Sjöbring, U., Björck, L., 1992. Structure of peptostreptococcal protein L and identification of a repeated immunoglobulin light chain-binding domain. J. Biol. Chem. 267, 12820–12825.

Kittler, S., Kopp, J., Veelenturf, P.G., Spadiut, O., Delvigne, F., Herwig, C., Slouka, C., 2020. The lazarus escherichia coli effect: recovery of productivity on glycerol/lactose mixed feed in continuous biomanufacturing. Front. Bioeng. Biotechnol. 8, 993.

Kittler, S., Besleaga, M., Ebner, J., Spadiut, O., 2021. Protein L—More Than Just an Affinity Ligand. Processes 9.

Kopp, J., Slouka, C., Ulonska, S., Kager, J., Fricke, J., Spadiut, O., Herwig, C., 2017. Impact of Glycerol as Carbon Source onto Specific Sugar and Inducer Uptake Rates and Inclusion Body Productivity in E. coli BL21(DE3). Bioeng. (Basel, Switz.) 5, 1.

Kopp, J., Zauner, F.B., Pell, A., Hausjell, J., Humer, D., Ebner, J., Herwig, C., Spadiut, O., Slouka, C., Pell, R., 2020. Development of a generic reversed-phase liquid chromatography method for protein quantification using analytical quality-by-design principles. J. Pharm. Biomed. Anal. 188, 113412.

Kröger, D., Liley, M., Schiweck, W., Skerra, A., Vogel, H., 1999. Immobilization of histidine-tagged proteins on gold surfaces using chelator thioalkanes. Biosens. Bioelectron. 14, 155–161.

Laemmli, U.K., 1970. Cleavage of structural proteins during the assembly of the head of bacteriophage T4. Nature 227, 680–685.

Ley, C., Holtmann, D., Mangold, K.-M., Schrader, J., 2011. Immobilization of histidine-tagged proteins on electrodes. Colloids Surf. B: Biointerfaces 88, 539–551.

Molin So Fau, -, Nygren, H., Nygren, H., Fau, -, Dolonius, L., Dolonius, L., 1978a. A new method for the study of glutaraldehyde-induced crosslinking properties in proteins with special reference to the reaction with amino groups. J. Histochem. Cytochem.: Off. J. Histochem. Soc. 26.

Moscetti, I., Cannistraro, S., Bizzarri, A.R., 2017. Surface plasmon resonance sensing of biorecognition interactions within the tumor suppressor p53 network. Sensors 17, 2680.

Nilson, B.H., Solomon, A., Björck, L., Akerström, B., 1992. Protein L from Peptostreptococcus magnus binds to the kappa light chain variable domain. J. Biol. Chem. 267, 2234–2239.

Nilson, B.H., Lögdberg, L., Kastern, W., Björck, L., Akerström, B., 1993. Purification of antibodies using protein L-binding framework structures in the light chain variable domain. J. Immunol. Methods 164, 33–40.

Nygren, H., Fau, -, Hansson, H.A., Hansson, H.A., 1981. Conjugation of horseradish peroxidase to staphylococcal protein A with benzoquinone, glutaraldehyde, or periodate as cross-linking reagents. The journal of histochemistry and cytochemistry: official journal of the Histochemistry. J. Histochem. Cytochem.: Off. J. Histochem. Soc. 29, 266–270.

PROTEIN-L, HIS, ⟨https://www.prospecbio.com/protein-l_his⟩ (accessed 02.07.2019).

Rodrigo, G., Gruvegård, M., Van Alstine, J.M., 2015. Antibody fragments and their purification by protein L affinity chromatography. Antibodies 4.

Rosenthal, M.E., Rojtman Ad Fau, -, Frank, E., Frank, E., 2012. Finegoldia magna (formerly Peptostreptococcus magnus): an overlooked etiology for toxic shock syndrome? Med. Hypotheses 79, 138–140.

Schwaighofer, A., Lendl, B., 2020. Chapter 3 - quantum cascade laser-based infrared transmission spectroscopy of proteins in solution. In: Ozaki, Y., Baranska, M., Lednev, I.K., Wood, B.R. (Eds.), Vibrational Spectroscopy in Protein Research. Academic Press, pp. 59–88.

Schwaighofer, A., Montemurro, M., Freitag, S., Kristament, C., Culzoni, M.J., Lendl, B., 2018. Beyond fourier transform infrared spectroscopy: external cavity quantum cascade laser-based mid-infrared transmission spectroscopy of proteins in the amide I and amide II region. Anal. Chem. 90, 7072–7079.

Shen, H., Schmuck, M., Pilz, I., Gilkes, N.R., Kilburn, D.G., Miller, R.C., Warren, R.A., 1991. Deletion of the linker connecting the catalytic and cellulose-binding domains of endoglucanase A (CenA) of Cellulomonas fimi alters its conformation and catalytic activity. J. Biol. Chem. 266, 11335–11340.

Shen, M., Rusling, J., Dixit, C.K., 2017. Site-selective orientated immobilization of antibodies and conjugates for immunodiagnostics development. Methods 116, 95–111.

Slouka, C., Kopp, J., Hutwimmer, S., Strahammer, M., Strohmer, D., Eitenberger, E., Schwaighofer, A., Herwig, C., 2018. Custom made inclusion bodies: impact of classical process parameters and physiological parameters on inclusion body quality attributes. Microb. Cell Factor. 17, 148-148.

So Fau, M., Nygren, H., Nygren, H., Fau, -, Dolonius, L., Dolonius, L., Fau, -, Hansson, H. A., Hansson, H.A., 1978b. A kinetic study of the reaction between glutaraldehyde and horseradish peroxidase. J. Histochem. Cytochem.: Off. J. Histochem. Soc. 26.

Sparks, R.P., Jenkins, J.L., Fratti, R., 2019. Use of surface plasmon resonance (SPR) to determine binding affinities and kinetic parameters between components important in fusion machinery. Methods Mol. Biol. 1860, 199–210.

Sultana, A., Lee, J.E., 2015. Measuring protein-protein and protein-nucleic acid interactions by biolayer interferometry. Curr. Protoc. Protein Sci. 79, 19.25.11-19.25.26.

Varadi, M., Anyango, S., Deshpande, M., Nair, S., Natassia, C., Yordanova, G., Yuan, D., Stroe, O., Wood, G., Laydon, A., Žídek, A., Green, T., Tunyasuvunakool, K., Petersen, S., Jumper, J., Clancy, E., Green, R., Vora, A., Lutfi, M., Figurnov, M., Cowie, A., Hobbs, N., Kohli, P., Kleywegt, G., Birney, E., Hassabis, D., Velankar, S., 2022. AlphaFold Protein Structure Database: massively expanding the structural coverage of protein-sequence space with high-accuracy models. Nucleic Acids Res. 50, D439–D444.

Wikstroem, M., Drakenberg, T., Forsen, S., Sjoebring, U., Bjoerck, L., 1994. Three-dimensional solution structure of an immunoglobulin light chain-binding domain of protein L. Comparison with the IgG-binding domains of protein G. Biochemistry 33, 14011–14017.

Zheng, Z., Chinnasamy, N., Morgan, R.A., 2012. Protein L: a novel reagent for the detection of Chimeric Antigen Receptor (CAR) expression by flow cytometry. J. Transl. Med. 10, 29.